COMMUNICATION

Ferroelectric and Dielectric Properties of Lead-free $K_{0.5}Bi_{0.5}TiO_3$-BiFeO$_3$ Ceramics

Jianxi Wen[1] **and Ge Wang**[1,*]

[1] Department of Materials, University of Manchester, Manchester M13 9PL, United Kingdom

Abstract

Lead-free (1-x)K$_{0.5}$Bi$_{0.5}$TiO$_3$-xBiFeO$_3$ ceramics with $x = 0.1$-0.4 were prepared by a conventional solid-state reaction. X-ray diffraction coupled with Rietveld refinement confirmed main perovskite phase with pseudo-cubic structure. Temperature-dependent dielectric measurements revealed broad dielectric anomalies and frequency dispersion, indicating relaxor behaviour. At 100 kHz, the highest room-temperature relative permittivity of 925 was obtained at $x = 0.2$. The highest maximum and remanent polarisation were obtained at $x = 0.3$ with 30 and 16 μC cm^{-2}, respectively. This work demonstrates a new lead-free solid solution for dielectric and ferroelectric applications.

Keywords: lead-free, KBT-BF, dielectric, ferroelectric, relaxor.

1 Introduction

Lead-based ferroelectric ceramics, particularly Pb(Zr,Ti)O$_3$ (PZT)-based materials, have been widely used in sensors, actuators, transducers and dielectric devices because of their excellent piezoelectric and ferroelectric properties [3]. However, the toxicity of lead and increasingly strict environmental regulations [2] have driven the development of lead-free alternatives capable of delivering comparable electric field-induced strains for actuator applications [1]. This has led to considerable interest in lead-free perovskite ceramics, especially Bi-contained and alkali-based systems, which can provide a strong polarisation response while avoiding the environmental and health concerns associated with Pb-based compounds.

Potassium bismuth titanate, K$_{0.5}$Bi$_{0.5}$TiO$_3$ (KBT), is an attractive lead-free ferroelectric owing to its tetragonal ferroelectric character, thermal stability and relatively high ferroelectric transition temperature, typically reported at approximately 380 °C [4]. Nevertheless, pure KBT is difficult to optimise as a dense, single-phase ceramic, partly because the volatility of K- and Bi-containing species during high-temperature processing can lead to non-stoichiometry, defect formation and increased dielectric loss [5, 6]. BiFeO$_3$ (BF) is another important lead-free perovskite, known for its intrinsically high transition temperature (830 °C) and large spontaneous polarisation (> 100 μC/cm^2) [6, 7]. Combining KBT with BF therefore offers a route to lead-free ceramics with improved thermal stability and enhanced polarisation

Submitted: 04 May 2026
Accepted: 13 June 2026
Published: 22 June 2026

Vol. 2, **No.** 2, 2026.
10.62762/JAEM.2026.712321

***Corresponding author:**
✉ Ge Wang
ge.wang@manchester.ac.uk

Citation
Wang, G., & Wen, J. (2026). Ferroelectric and Dielectric Properties of Lead-free $K_{0.5}Bi_{0.5}TiO_3$-BiFeO$_3$ Ceramics. *Journal of Advanced Electronic Materials*, 2(2), 51–57.

© 2026 by the Authors. Published by Institute of Central Computation and Knowledge. This is an open access article under the CC BY license (https://creativecommons.org/licenses/by/4.0/).

response [8, 9].

The functional potential of KBT–BF ceramics is closely linked to their composition-dependent phase behaviour. A composition of 0.4KBT–0.6BF has been identified as being close to the morphotropic phase boundary, showing a remanent polarisation, P_r, of about 52 μC cm^{-2} and retaining piezoelectric properties up to 300 °C [8]. This combination of large polarisation and high-temperature stability suggests that KBT–BF is a promising parent system for further compositional modification aimed at dielectric and capacitor-related applications. More recently, Wang et al. [10] investigated the energy-storage performance of 0.6KBT–0.4BF-based ceramics through defect engineering and relaxor tuning, reporting a high maximum polarisation (P_{max}) of approximately 60 μC cm^{-2} and a remanent polarisation (P_r) of 35 μC cm^{-2}; however, performance was found to be constrained by Fe-valence fluctuation and Bi_2O_3 volatilisation during sintering, which increase oxygen-vacancy concentration and leakage current. Fisher et al. [6] reported that KBT–BF ceramics are difficult to sinter to high density and therefore investigated reactive sintering as an alternative route for preparing KBT–BF ceramics. These issues are closely related to Bi/K volatilisation, oxygen vacancies and mixed Fe valence states, which can promote leakage current and extrinsic conductivity [5, 6, 11].

Mn addition has been reported to suppress conductivity and reduce dielectric loss by modifying the defect chemistry of BF-containing perovskites and related Bi-based perovskites [6, 12]. This is important for obtaining dielectric and ferroelectric behaviour. In 0.4KBT–0.6BF, the addition of 0.5 mol% MnO reduced dc conductivity by approximately two and three orders of magnitude and produced a well-defined Arrhenius activation energy of 1.21 eV, consistent with Mn-induced acceptor defect levels and suppression of Fe-related polaron conduction [6]. A similar Mn-induced conductivity suppression mechanism has also been reported in related Bi-based perovskite systems such as $BiFeO_3$–$BaTiO_3$, where Mn acts as an acceptor dopant to reduce leakage current [13]. Similarly, 1 at% Mn-doped NBT–BT single crystals showed enhanced resistivity and improved electromechanical properties, with reported d_{33}, k_t and k_{31} values of 483 pC N^{-1}, 0.556 and 0.397 respectively [12]. In this work, (1-x)$K_{0.5}Bi_{0.5}TiO_3$–$x$$BiFeO_3$ ceramics modified with small amounts of Mn were prepared by a conventional solid-state reaction route. The phase structure, dielectric properties and ferroelectric response were investigated to study the composition–structure–property relationship.

2 Experimental procedure

Lead-free (1-x)$K_{0.5}Bi_{0.5}TiO_3$–$x$$BiFeO_3$ (KBT–xBF) ceramics, where x = 0.1, 0.2, 0.3 and 0.4, were prepared by a conventional solid-state reaction method. Analytical-grade K_2CO_3 ($\geq$ 99.0%, Sigma-Aldrich), Bi_2O_3 ($\geq$ 99.9%, Thermo scientific), TiO_2 ($\geq$ 99.9%, Sigma-Aldrich), Fe_2O_3 ($\geq$ 98%, Thermo scientific) and Mn_2O_3 (99%, Sigma-Aldrich) were used as starting raw materials. A small amount of 0.1 wt% Mn was added to suppress the extrinsic conductivity. All chemicals were mixed stoichiometrically and homogenised by vibration milling in propan-2-ol for 24 h using yttria-stabilised zirconia milling media. The resulting slurry was dried overnight, and the dried powder mixture was calcined at 900 °C for 4 h. The calcined powders were subsequently re-milled. After drying, the powders were mixed with 10 wt% polyvinyl alcohol (PVA) binder and uniaxially pressed into pellets with a diameter of approximately 10 mm under a pressure of 150–200 MPa. The green pellets were heated at 550 °C for 2 h to remove the binder, followed by sintering at 1065–1075 °C for 2 h with a heating rate of 3 °C min^{-1}.

Phase formation and crystallographic characteristics of the sintered ceramics were examined by X-ray diffraction (XRD). Prior to XRD measurements, the sintered pellets were crushed into fine powders. Diffraction patterns were collected using a PANalytical X'Pert PRO PW3050/60 diffractometer with Cu Kα radiation (λ = 1.54 Å). Data were recorded over a 2θ range of 10–90° with a step size of 0.0167° and a counting time of 139.7 s per step. The XRD data were used to identify the phase structure and assess possible phase evolution or lattice distortion in the KBT–BF ceramics. Pattern refinement and peak fitting of the XRD data were carried out using TOPAS 6 to determine the crystallographic parameters of the sintered ceramics.

For dielectric and ferroelectric measurements, both sides of the sintered pellets were coated with silver paste (Sunchemical, UK) as electrodes and fired at 500 °C for 30 min. Excess silver electrodes around the pellet edges were carefully removed to avoid electrical short-circuiting. The electroded samples were placed between platinum wires in a Carbolite Gero furnace and connected to an HP 4284A Precision LCR meter. Temperature-dependent dielectric measurements

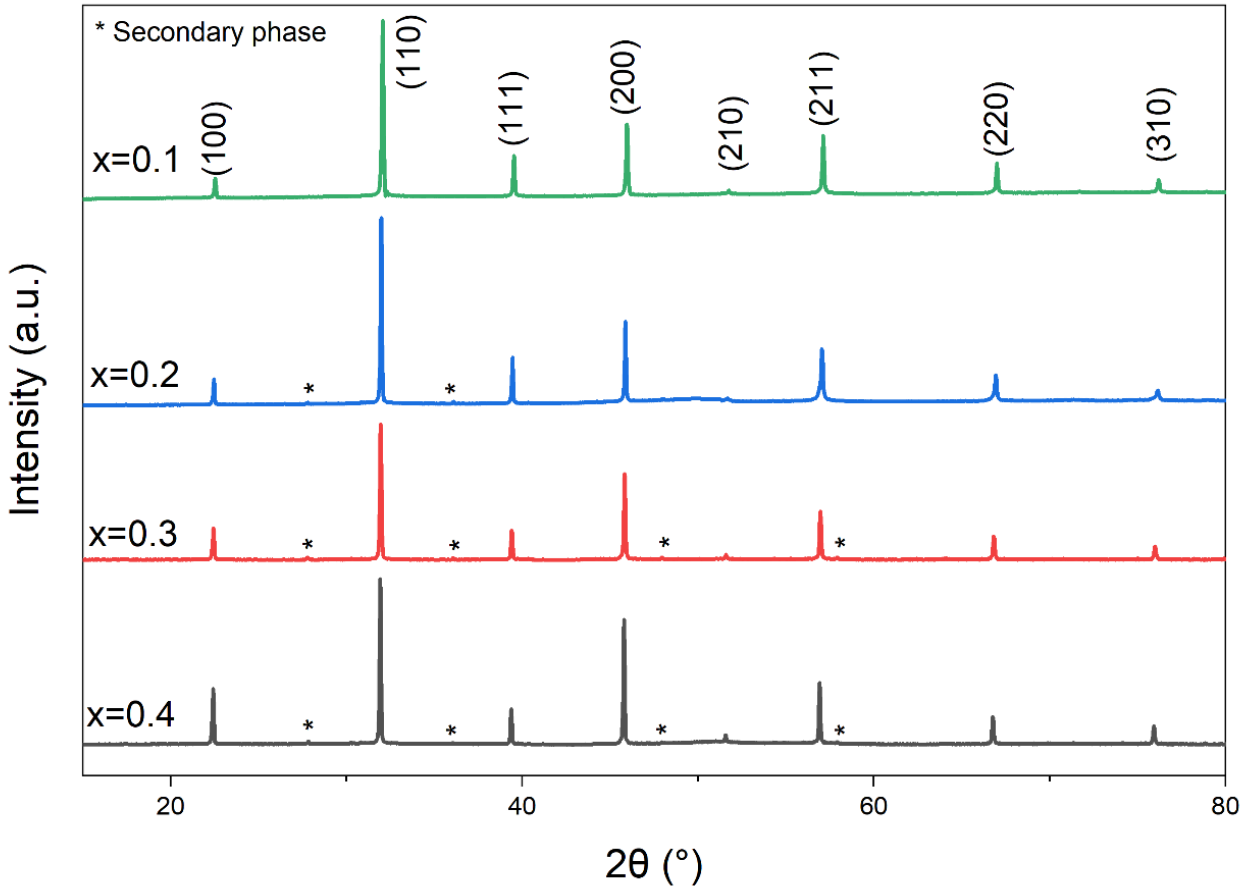

Figure 1. XRD patterns of KBT-xBF ceramics, where $x = 0.1$–0.4.

Table 1. Lattice parameter of KBT–xBF ceramics, where $x = 0.1$–0.4.

Composition	$x = 0.1$	$x = 0.2$	$x = 0.3$	$x = 0.4$
$a = b = c$ (Å)	3.9497(2)	3.9523(1)	3.9558(2)	3.9588(1)

were performed from 25 to 550 °C at a heating rate of 1 °C min^{-1}, at frequencies of 1, 10 and 100 kHz. The relative permittivity was calculated from the measured capacitance using the standard parallel-plate capacitor relationship, and the dielectric constant and dielectric loss were evaluated as functions of temperature and frequency. The ferroelectric polarisation–electric field (P–E) response was characterised under a sinusoidal electric-field waveform, with the instantaneous polarisation determined by integrating the current response as a function of time [14]. The ceramic samples were measured at a frequency of 1 Hz.

3 Results and Discussion

Figure 1 presents the X-ray diffraction patterns of the KBT–xBF ceramics ($x = 0.1$–0.4). The principal diffraction peaks can be indexed to a pseudo-cubic perovskite structure. This indicates that the perovskite phase is retained across the investigated composition range. A few weak XRD peaks are also present, which may be associated with impurity phases caused by volatilisation of K- and Bi-containing species during high-temperature sintering. Such volatilisation can produce local non-stoichiometry and favour the formation of minor secondary phases [15–17].

Rietveld refinement was performed using Topas, and best fit was obtained using a cubic $Pm\bar{3}m$ model. Within the present XRD pattern, no pronounced peak splitting or symmetry change was observed with increasing BF content. The samples can therefore be described using an average pseudo-cubic structure. As

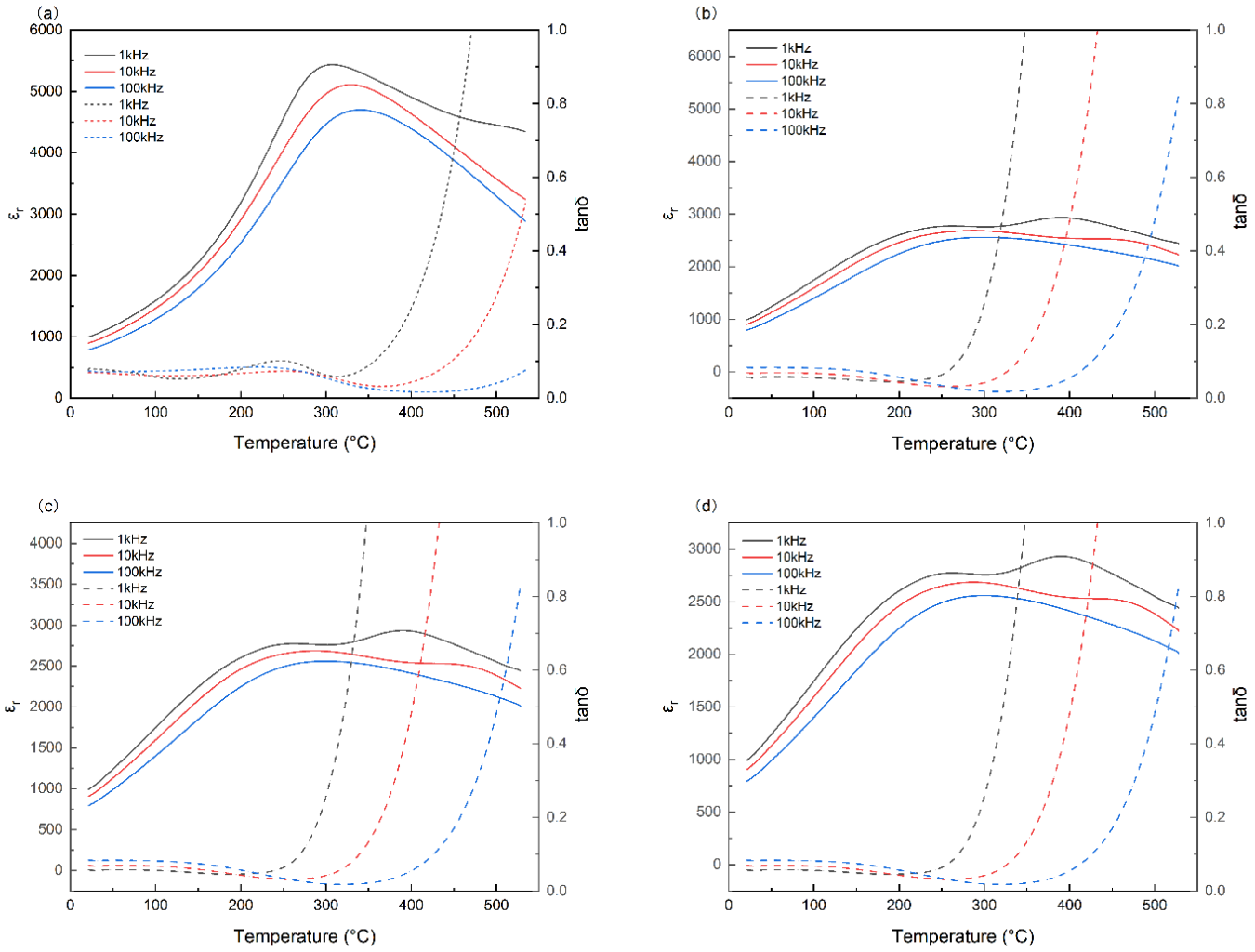

Figure 2. Temperature-dependent relative permittivity (ε_r) and dielectric loss ($\tan\delta$) of KBT–xBF measured at frequencies of 1, 10 and 100 kHz: (a) $x = 0.1$, (b) $x = 0.2$, (c) $x = 0.3$ and (d) $x = 0.4$.

summarised in Table 1, the refined lattice parameter increases gradually from 3.9497(2) Å for $x = 0.1$ to 3.9588(1) Å for $x = 0.4$. This trend indicates expansion of the pseudo-cubic unit cell with increasing BF content. The increase in pseudo-cubic lattice parameter with increasing BF content was rationalised using Shannon effective ionic radii. The ionic radius of high-spin Fe^{3+} (0.645 Å, CN=6) is larger than that of Ti^{4+} (0.605 Å, CN=6) [18]. The substitution of the larger Fe^{3+} for Ti^{4+} at the B-site leads to an increase in the average B-site ionic radii. Therefore, the lattice expansion is consistent with compositional modification and the incorporation of Fe into the B-site.

Figure 2 shows the temperature-dependent dielectric permittivity (ε_r) and dielectric loss ($\tan\delta$) of KBT–xBF ceramics measured at 1, 10 and 100 kHz. All compositions exhibit broad dielectric anomalies and frequency dispersion, indicating relaxor behaviour. This behaviour is likely related to compositional disorder on both the A-site and B-site sublattices, which can generate local structural heterogeneity and polar nano-regions. The coexistence of K^+/Bi^{3+} on the A-site and Ti^{4+}/Fe^{3+} on the B-site is expected to disrupt long-range ferroelectric order and broaden the dielectric transition. At lower temperatures, ε_r increases gradually with temperature for all compositions. On further heating, broad maxima are observed, followed by a decrease in ε_r at higher temperatures. The dielectric loss remains comparatively low at lower temperatures but increases rapidly at elevated temperatures, particularly at lower frequency. This increase in $\tan\delta$ is characteristic of thermally activated charge transport and may be associated with oxygen vacancies, Bi/K volatilisation-induced defects and Fe-related electronic

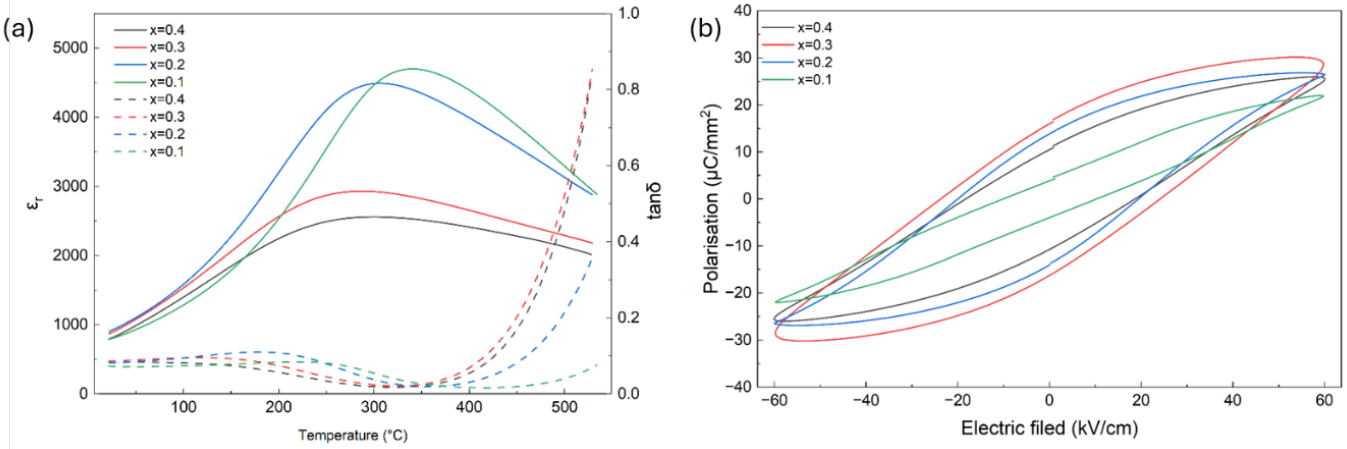

Figure 3. (a) Temperature-dependent relative permittivity (ε_r) and dielectric loss ($\tan\delta$) of KBT–xBF measured at 100 kHz; (b) Bipolar P–E loops for KBT–xBF at 60 kV cm^{-1}.

conduction.

Figure 3(a) compares the dielectric response at 100 kHz. At room temperature, the permittivity remains in the range of approximately 803–925, with $x = 0.2$ showing the highest value ($\varepsilon_r = 925$), while $x = 0.1$ gives the lowest value ($\varepsilon_r = 803$). The room-temperature dielectric loss is relatively low ($< 10\%$), with $\tan\delta$ values in the range of 0.073–0.087 across all compositions. With increasing temperature, all compositions exhibit relatively broad dielectric curve rather than a sharp transition, suggesting relaxor behaviour. The maximum permittivity decreases gradually with increasing x, from 4700 for $x = 0.1$ to 2559 for $x = 0.4$. At elevated temperatures, dielectric loss increases markedly at 400 °C for $x = 0.2$–0.4.

Figure 3(b) shows the bipolar P–E hysteresis loops of the KBT–xBF ceramics at 60 kV cm^{-1}. The P–E loop for $x = 0.1$ is very slim with $P_{max} = 22$ μC cm^{-2} and $P_r = 4$ μC cm^{-2}. The other three compositions show higher P_{max} and P_r values than $x = 0.1$, with the highest value obtained at $x = 0.3$, as detailed in Table 2. The P_{max} increases from 22 μC cm^{-2} for $x = 0.1$ to 30 μC cm^{-2} for $x = 0.3$ and then decreases to 26 μC cm^{-2} for $x = 0.4$. A similar trend is also observed for the P_r. These results indicate that the composition with $x = 0.3$ exhibits the highest polarisation. However, slight round edges were observed at the highest field for $x = 0.3$, indicating a conductive behaviour that is possibly due to the formation of oxygen vacancies.

4 Conclusion

(1-x)$K_{0.5}Bi_{0.5}TiO_3$–$x$$BiFeO_3$ ceramics with $x = 0.1$–0.4 were prepared by a conventional solid-state reaction.

Table 2. Important parameters from P–E loops for KBT–xBF at 60 kV cm^{-1}.

Composition	$\lvert P_{max}\rvert$ (μCcm^{-2})	$\lvert P_r\rvert$ (μCcm^{-2})	$\lvert E_c\rvert$ (kVcm^{-1})
0.9KBT–0.1BF	22	4	10
0.8KBT–0.2BF	27	14	20
0.7KBT–0.3BF	30	16	24
0.6KBT–0.4BF	26	11	18

XRD analysis confirmed that the main reflection is perovskite pseudo-cubic structure, with weak secondary reflections attributed to minor impurity phases associated with K/Bi volatilisation during sintering. The refined pseudo-cubic lattice parameter increased from 3.9497(2) Å for $x = 0.1$ to 3.9588(1) Å for $x = 0.4$, indicating expansion of the perovskite unit cell with increasing BF content. Dielectric measurements revealed broad anomalies and frequency-dependent behaviour, consistent with a diffuse and relaxor-like response. At 100 kHz, the room-temperature relative permittivity was approximately 803–925, while $\tan\delta$ remained between 0.073 and 0.087. Ferroelectric P–E loop results showed slim hysteresis loops, indicating relaxor behaviour. The highest polarisation was obtained for $x = 0.3$, with $P_{max} = 30$ μC cm^{-2}, $P_r = 16$ μC cm^{-2} and $E_c = 24$ kV cm^{-1}. Overall, this work demonstrates a fundamental composition–structure–property relationship in KBT–BF ceramics.

Data Availability Statement

Data will be made available on request.

Funding

The authors gratefully acknowledge financial support from the Dame Kathleen Ollerenshaw Fellowship at The University of Manchester and from the Engineering and Physical Sciences Research Council (EPSRC) under Grant EP/Z536003/1.

Conflicts of Interest

Ge Wang served as an Associate Editor of the *Journal of Advanced Electronic Materials* at the time of manuscript submission. To ensure the integrity of the peer-review process, Ge Wang was not involved in the editorial handling, peer review, or decision-making process for this manuscript, which was handled independently by another editor. The remaining authors declare no conflicts of interest.

AI Use Statement

The authors declare that no generative AI was used in the preparation of this manuscript.

Ethical Approval and Consent to Participate

Not applicable.

References

[1] Jo, W., Dittmer, R., Acosta, M., Zang, J., Groh, C., Sapper, E., ... & Rödel, J. (2012). Giant electric-field-induced strains in lead-free ceramics for actuator applications–status and perspective. *Journal of Electroceramics, 29*(1), 71-93. [CrossRef]

[2] Bell, A. J., & Deubzer, O. (2018). Lead-free piezoelectrics—The environmental and regulatory issues. *Mrs bulletin, 43*(8), 581-587. [CrossRef]

[3] Rödel, J., Jo, W., Seifert, K. T., Anton, E. M., Granzow, T., & Damjanovic, D. (2009). Perspective on the development of lead-free piezoceramics. *Journal of the American Ceramic Society, 92*(6), 1153-1177. [CrossRef]

[4] Hiruma, Y., Aoyagi, R., Nagata, H., & Takenaka, T. (2005). Ferroelectric and piezoelectric properties of (Bi1/2K1/2) TiO3 ceramics. *Japanese journal of applied physics, 44*(7R), 5040. [CrossRef]

[5] König, J., Spreitzer, M., Jančar, B., Suvorov, D., Samardžija, Z., & Popovič, A. (2009). The thermal decomposition of K0. 5Bi0. 5TiO3 ceramics. *Journal of the European Ceramic Society, 29*(9), 1695-1701. [CrossRef]

[6] Fisher, J. G., Kim, M. G., Kim, D., Cha, S. J., Vu, H. V., Nguyen, D., ... & Kim, M. H. (2015). Reactive sintering of (K0. 5Bi0. 5) TiO3-BiFeO3 lead-free piezoelectric ceramics. *Journal of the Korean Physical Society, 66*(9), 1426-1438. [CrossRef]

[7] Lebeugle, D., Colson, D., Forget, A., & Viret, M. (2007). Very large spontaneous electric polarization in BiFeO3 single crystals at room temperature and its evolution under cycling fields. *Applied Physics Letters, 91*(2), 022907. [CrossRef]

[8] Matsuo, H., Kitanaka, Y., Noguchi, Y., Miyayama, M., Moriwake, H., Kuwabara, A., & Tanaka, I. (2010). Structural and piezoelectric properties of high-density (Bi0.5K0.5)TiO3–BiFeO3 ceramics. *Journal of Applied Physics, 108*(10), 104103. [CrossRef]

[9] Morozov, M. I., Einarsrud, M. A., Grande, T., & Damjanovic, D. (2012). Lead-free relaxor-like 0.75 Bi0. 5K0. 5TiO3–0.25 BiFeO3 ceramics with large electric field-induced strain. *Ferroelectrics, 439*(1), 88-94. [CrossRef]

[10] Wang, H., Li, E., Wei, K., Li, H., Xing, M., & Zhong, C. (2022). Significantly Enhanced Energy Storage Performance in High Hardness BKT-Based Ceramic via Defect Engineering and Relaxor Tuning. *ACS Applied Materials & Interfaces, 14*(48), 54021–54033. [CrossRef]

[11] Wefring, E. T., Einarsrud, M. A., & Grande, T. (2015). Electrical conductivity and thermopower of (1-x) BiFeO 3-x Bi 0.5 K 0.5 TiO 3 (x= 0.1, 0.2) ceramics near the ferroelectric to paraelectric phase transition. *Physical Chemistry Chemical Physics, 17*(14), 9420-9428. [CrossRef]

[12] Zhang, Q., Zhang, Y., Wang, F., Wang, Y., Lin, D., Zhao, X., ... & Viehland, D. (2009). Enhanced piezoelectric and ferroelectric properties in Mn-doped Na0. 5Bi0. 5TiO3–BaTiO3 single crystals. *Applied Physics Letters, 95*(10), 102904. [CrossRef]

[13] Leontsev, S. O., & Eitel, R. E. (2009). Dielectric and piezoelectric properties in Mn-modified (1-x) BiFeO3-xBaTiO3 ceramics. *Journal of the American Ceramic Society, 92*(12), 2957-2961. [CrossRef]

[14] Stewart, M., Cain, M. G., & Hall, D. A. (1999). Ferroelectric hysteresis measurement and analysis. *NPL Report CMMT(A)152*. National Physical Laboratory.

[15] König, J., & Suvorov, D. (2015). Evolution of the electrical properties of K0. 5Bi0. 5TiO3 as a result of prolonged sintering. *Journal of the European Ceramic Society, 35*(10), 2791-2799. [CrossRef]

[16] Suchanicz, J., Kania, A., Czaja, P., Budziak, A., & Niewiadomski, A. (2018). Structural, thermal, dielectric and ferroelectric properties of K0. 5Bi0. 5TiO3 ceramics. *Journal of the European Ceramic Society, 38*(2), 567-574. [CrossRef]

[17] Zaremba, T. (2003). Application of thermal analysis to study of the synthesis of K 0.5 Bi 0.5 Tio 3 ferroelectric. *Journal of thermal analysis and calorimetry, 74*(2), 653-658. [CrossRef]

[18] Shannon, R. D. (1976). Revised effective ionic radii and systematic studies of interatomic distances in halides and chalcogenides. *Foundations of Crystallography*, *32*(5), 751-767. [CrossRef]

Jianxi Wen is a PhD researcher at The University of Manchester with a background in materials science and engineering. He obtained a Bachelor's degree in Materials Science with Honours from Monash University in 2021 and an MSc in Advanced Engineering Materials from The University of Manchester in 2023. His research focuses on the structure–composition–property relationships in lead-free functional ceramics. He specialises in ceramic processing and advanced structural and electrical characterisation techniques for environmentally friendly electroceramic materials. (Email: jianxi.wen@manchester.ac.uk)

Ge Wang obtained a PhD (2016) from the University of Manchester. He worked as a postdoctoral research associate at the University of Sheffield (2017-2022) and was awarded a Dame Kathleen Ollerenshaw Fellowship (2022) at the Department of Materials, The University of Manchester (UoM). His independent research at UoM is focused on the development (synthesis and characterisation) of high-performance functional ceramics, including dielectric, piezoelectric and solid-state electrolytes, using skillset ranging from crystal chemistry and crystallography to advanced processing of ceramics and prototype devices. He published 60+ peer-reviewed articles with a H-index of 33 and 6000+ citations (Google Scholar). He is currently the deputy research lead for Nano and Functional Materials at the Department of Materials, a Fellow of the Higher Education Academy (FHEA) and a professional member of Royal Society of Chemistry (MRSC). His work has been funded by the Engineering and Physical Sciences Research Council (EPSRC), the Royal Society, and the Royal Society of Chemistry. (Email: ge.wang@manchester.ac.uk)